The International Journal of Biochemistry & Cell Biology 79 (2016) 128–138

Contents lists available at ScienceDirect

The International Journal of Biochemistry & Cell Biology

journal homepage: www.elsevier.com/locate/biocel

Circumventing the Crabtree Effect: A method to induce lactate consumption and increase oxidative phosphorylation in cell culture

Alexandra I. Mot[a], Jeffrey R. Liddell[a], Anthony R. White[a,b], Peter J. Crouch[a,b,*]

[a] Department of Pathology, University of Melbourne, Australia
[b] Florey Institute of Neuroscience and Mental Health, University of Melbourne, Australia

ARTICLE INFO

Article history:
Received 26 April 2016
Received in revised form 15 August 2016
Accepted 29 August 2016
Available online 30 August 2016

Keywords:
Cell culture
Mitochondria
Lactate
Oxidative phosphorylation (OXPHOS)
Electron transport chain (ETC)

ABSTRACT

Most cells grown in glucose-containing medium generate almost all their ATP via glycolysis despite abundant oxygen supply and functional mitochondria, a phenomenon known as the Crabtree effect. By contrast, most cells within the body rely on mitochondrial oxidative phosphorylation (OXPHOS) to generate the bulk of their energy supply. Thus, when utilising the accessibility of cell culture to elucidate fundamental elements of mitochondria in health and disease, it is advantageous to adopt culture conditions under which the cells have greater reliance upon OXPHOS for the supply of their energy needs. Substituting galactose for glucose in the culture medium can provide these conditions, but additional benefit can be gained from alternate *in vitro* models. Herein we describe culture conditions in which complete autonomous depletion of medium glucose induces a lactate-consuming phase marked by increased Mito-Tracker Deep Red staining intensity, increased expression of Kreb's cycle proteins, increased expression of electron transport chain subunits, and increased sensitivity to the OXPHOS inhibitor rotenone. We propose these culture conditions represent an alternate accessible model for the *in vitro* study of cellular processes and diseases involving the mitochondrion without limitations incurred via the Crabtree effect.

1. Introduction

Glycolysis is an inefficient mechanism for generating ATP relative to mitochondrial oxidative phosphorylation (OXPHOS) (Lunt and Vander Heiden, 2011), and most cells within the body therefore rely on OXPHOS to meet the bulk of their energy requirements. However, the presence of glucose in commonly used cell culture conditions favours glycolysis over OXPHOS due to allosteric modulation of glycolytic enzymes by glucose (Rodriguez-Enriquez et al., 2001) and the binding of hexokinase to mitochondrial porin which accelerates glycolysis (Golshani-Hebroni and Bessman, 1997). As a consequence, most cells grown in glucose-containing medium generate almost all their ATP via glycolysis despite abundant oxygen supply and the presence of functional mitochondria, a phenomenon known as the Crabtree effect (Crabtree, 1929). This phenomenon is not restricted to cells cultured in high glucose-containing medium (~20 mM) but also occurs in cells cultured in low glucose-containing (~5 mM) medium (Rodriguez-Enriquez et al., 2001).

To enhance extrapolation from cell culture experiments to *in vivo* conditions pertaining to energetically demanding cells and/or conditions arising from decreased mitochondrial function, it is therefore useful to adapt the cell culture environment such that cells are less glycolytic and more dependent on OXPHOS. One way of achieving this is by substituting glucose in the culture medium with galactose, usually at concentrations of 5–10 mM (Aguer et al., 2011; Allen et al., 2014; Bird et al., 2014; Dott et al., 2014; Marroquin et al., 2007; Robinson et al., 1992; Warburg et al., 1967). The slow oxidation of galactose to pyruvate via glycolysis forces cells to rely on mitochondrial OXPHOS to generate sufficient ATP for survival (Dott et al., 2014). Other carbohydrates including fructose and maltose have been used to replace medium glucose for the purpose of stabilising medium pH (Imamura et al., 1982) but these models have not been widely utilised.

To date the galactose model is the most widely used way to circumvent the Crabtree effect. However, limitations of this model are

Abbreviations: AMPK, α5′-adenosine monophosphate-activated protein kinase alpha; ATP5A, ATP synthase subunit alpha; BCA, bicinchoninic acid; FCCP, carbonyl cyanide *p*-(trifluoromethoxy) phenylhydrazone; COX5B, cytochrome c oxidase subunit 5B; 2-DG, 2-deoxyglucose; GAPDH, glyceraldehyde-3-phosphate dehydrogenase; OXPHOS, oxidative phosphorylation; PCNA, proliferating cell nuclear antigen; pMEFs, primary mouse embryonic fibroblasts; SDHB, succinate dehydrogenase subunit B; SOD1, superoxide dismutase 1; SOD2, superoxide dismutase 2; TOM20, mitochondrial import receptor subunit TOM20 homolog.

* Corresponding author at: Department of Pathology, University of Melbourne, 3010, Melbourne, Australia.
E-mail address: pjcrouch@unimelb.edu.au (P.J. Crouch).

http://dx.doi.org/10.1016/j.biocel.2016.08.029

associated with increased cellular metabolic stress and an accelerated ageing phenotype (Aguer et al., 2011; Barker et al., 1999; Choi et al., 2013; Coban et al., 2014; Li et al., 2014) and the fact that some cell types are unable to utilise galactose (Elkalaf et al., 2013). Additional benefit can therefore be gained from alternate approaches to overcome limitations associated with the Crabtree effect. Herein we describe culture conditions in which complete autonomous depletion of medium glucose forces cells to utilise lactate via mitochondrial OXPHOS to supply their energy needs. These conditions represent an alternate accessible model for the *in vitro* study of cellular processes and diseases involving the mitochondrion without limitations incurred via the Crabtree effect.

2. Materials and methods

2.1. Materials

Cell culture reagents were from Life Technologies and chemicals were from Sigma-Aldrich unless otherwise specified.

2.2. Cell culture conditions

Primary mouse embryonic fibroblasts (pMEFs) were obtained from E14 C57BL/6 mice as previously described (Garfield, 2010). At passage 1 cells were frozen and stored in liquid nitrogen. For each experiment cells were thawed then allowed to reach confluency, then passaged and seeded into 24-well plates (Nunc) at 1×10^4 cells/cm^2 in DMEM containing 3.5 mM glucose and supplemented with 10% (v/v) foetal bovine serum, 50 U/mL penicillin, 50 μg/mL streptomycin, 1 mM L-glutamine, and 9.7 mM mannitol (Ajax Finechem). Cultures were maintained at 37 °C in a humidified incubator with 5% CO_2.

Primary adult human fibroblasts were obtained from superficial skin biopsies of the right inner forearm of a healthy person as previously reported (Solski et al., 2012). All culture conditions were as described above for the pMEFs.

Primary mouse brain astrocytes were obtained from new born C57BL/6 pups as previously described (Hare et al., 2013). Cells were seeded into 48-well plates at 15×10^4 cells/cm^2 and allowed to reach maturity until day 15. Experiments were commenced on day 15 (thereafter referred to as experimental day 0) when the medium was replaced with DMEM containing 5.0 mM glucose and supplemented with 10% (v/v) foetal bovine serum, 50 U/mL penicillin, and 50 μg/mL streptomycin. Cultures were maintained at 37 °C in a humidified incubator with 10% CO_2.

These three cell types were chosen based on their versatility to manipulations in culture conditions. For all cell types the volume of media used was equivalent to 20 mL per T75 flask (266 μL/cm^2). All mouse work was approved by the University of Melbourne Biosciences Animal Ethics Committee. All human cell work was approved by the University of Melbourne Biosciences Human Ethics Committee.

2.3. Lactate and glucose content of cell culture medium

Lactate and glucose levels in the cell culture medium were determined using methods based on those previously described (Liddell et al., 2009). Aliquots of medium were collected from the cell cultures at the start of the culture period (day 0) then further aliquots collected once daily for 7 days (pMEFs) or 13 days (human fibroblasts). For astrocyte cultures medium aliquots were collected on days 0, 0.25, 1, and 5. Modifications made to the protocols described by Liddell et al. (2009) involved the use of glucose and lactate standard curves instead of extinction coefficients.

2.4. BCA assay for quantification of protein content

Total protein levels within each well of the culture plates were measured at each medium collection time point (once daily, on days 0–7) for the pMEFs. For all cell types protein levels were measured at the completion of all 2-deoxyglucose (2-DG) or rotenone treatments. Results are expressed relative to vehicle control treated cells to account for differences in cell confluency between glucose-consuming and lactate-consuming phases. Following medium collection, cells were washed twice with chilled PBS. Protein was solubilised using 300 μL per well of 100 mM NaOH and incubated on an orbital shaker at room temperature for 2 h. Protein concentration was measured using a Bicinchoninic Acid (BCA) Assay Kit (Thermo Scientific) by comparison to a bovine serum albumin standard curve, as per manufacturer instructions. While protein content is influenced by a multitude of factors, robust changes in total cellular protein are a good indicator of both cell proliferation and cell viability (Engelhard et al., 1991; Vichai and Kirtikara, 2006).

2.5. Phase contrast microscopy

Phase contrast microscopy was used to monitor changes in pMEF confluency and morphology daily during the experiment (days 0–7). Representative images of the cells were taken using a light microscope and a Canon Powershot A2300 digital camera on day 1 (glucose-consuming phase) and day 5 (lactate-consuming phase).

2.6. Western blotting for protein analyses

pMEFs grown in T75 flasks (Nunc) were pelleted (720 RCF, 3 min) and lysed in PhosphoSafe Extraction Buffer (Merck) supplemented with 1 mM phenylmethyl sulphonyl fluoride (PMSF) and 1.6 mM deoxyribonuclease I from bovine pancreas (DNase I, Roche). Following centrifugation (15,000 RCF, 3 min), lysates at equal protein concentration were mixed with 4 x gel loading buffer [250 mM Tris, 20% (v/v) glycerol, 8% (w/v) SDS, 2% (v/v) β-mercaptoethanol, 0.01% (w/v) bromophenol blue] then heated at 95 °C for 5 min. Denatured and reduced proteins were separated on 4–12% Bis Tris gels (NuPage) at 200 V for 42 min. Resolved proteins were transferred onto PVDF membranes at 20 V for 7 min using the iBlot transfer system (Invitrogen). PVDF membranes were blocked with PBST [PBS supplemented with 0.05% (v/v) Tween-20] containing 4% (w/v) skim milk powder. Membranes were incubated with primary antibody overnight at 4 °C then secondary antibody for 2 h at room temperature before visualising chemiluminescence of protein bands using ECL Advance (GE Healthcare) and a MicroChemi imager (DNR Bio-Imaging Systems). Primary antibodies to proliferating cell nuclear antigen (Cell Signaling #2586, 1:1500), citrate synthase (Abcam #ab96600, 1:800), cytochrome c oxidase subunit 5 B (Abcam #ab180136, 1:600), ATP synthase subunit alpha (Abcam #ab176569, 1:600), succinate dehydrogenase subunit B (Abcam #ab175225, 1:600), mitochondrial import receptor subunit TOM20 homolog (Protein Tech #11802-1-AP, 1:600), superoxide dismutase 2 (Abcam #ab13533, 1:5000), superoxide dismutase 1 (Abnova #PAB0725, 1:2000), phospho(Thr172)-5′-adenosine monophosphate-activated protein kinase alpha (Cell Signaling #2535, 1:400), 5′-adenosine monophosphate-activated protein kinase alpha (Cell Signaling #2532, 1:600), and glyceraldehyde-3-phosphate dehydrogenase (Cell Signaling #2118, 1:5000) were used. HRP-linked anti-rabbit IgG (Cell Signaling #7074, 1:5000) and HRP-linked anti-mouse IgG (Cell Signaling #7076, 1:5000) secondary antibodies were used. Relative abundance of proteins was determined using ImageJ 1.38 × software.

2.7. Fluorescence microscopy

pMEFs on coverslips were stained with the mitochondrial-specific dye MitoTracker Deep Red FM (Molecular Probes #M22426) or the primary antibody to mitochondrial import receptor subunit TOM20 homolog (TOM20, ProteinTech #11802-1-AP) on day 1 (glucose-consuming phase) and day 5 (lactate-consuming phase). Existing medium was supplemented with 500 nM MitoTracker Deep Red for 20 min at 37 °C in a humidified incubator with 5% CO_2. Cells were then fixed in 4% (w/v) paraformaldehyde (Electron Microscopy Sciences) for 20 min at room temperature. Fixed cells were permeabilised in 0.2% (v/v) Triton X-100 for 10 min at room temperature. Following blocking in PBS supplemented with 0.3% (v/v) Triton X-100 and 1% (w/v) bovine serum albumin, cells were incubated with primary TOM20 antibody (overnight at 4 °C), followed by fluorescently-tagged secondary anti-rabbit Alexa Fluor 568 antibody for 2 h at room temperature. All cells were stained with the nuclear stain DAPI (5 min at room temperature). MitoTracker Deep Red stained cells were imaged by taking single 1.0 μm thick images using a confocal microscope (Zeiss LSM Meta) and Zen imaging software. TOM20 stained cells were imaged using an AxioCam HR camera mounted onto a Leica Inverted Fluorescence microscope. Specificity of TOM20 mitochondrial staining was confirmed using confocal microscopy. To allow for quantitative comparisons between days 1 and 5 to be made, all coverslips were imaged using identical exposure times and laser power settings. Staining intensity (per cellular area) was obtained using ImageJ 1.38 × software. Briefly, cell nuclei masks (based on DAPI staining) were subtracted from total cellular area masks, after which staining intensity for the cytoplasmic area was quantified. To confirm that mitochondrial accumulation of MitoTracker Deep Red is dependent on mitochondrial membrane potential, pMEFs were treated with the mitochondrial depolarisation compound carbonyl cyanide *p*-(trifluoromethoxy) phenylhydrazone (FCCP) at 5 μM for 15 min in existing medium prior to incubation with MitoTracker Deep Red as above. Cells were then co-stained with TOM20 antibody and fluorescently-tagged secondary Alexa Fluor 488 antibody. All other aspects were as above, except that MitoTracker Deep Red staining intensity within mitochondria was quantified using TOM20 to generate a mask of the mitochondrial area.

2.8. Cell treatments with metabolic inhibitors

pMEFs were treated with the glycolysis inhibitor 2-deoxyglucose (2-DG; 5 mM) or vehicle control for 24 h on day 1 (glucose-consuming phase) and day 5 (lactate-consuming phase). All cell types were treated with the mitochondrial complex I inhibitor rotenone at concentrations and treatment durations optimised for each cell type. pMEFs were treated with 100 μM rotenone for 4 h on days 1 and 5. Astrocytes were treated with 50 nM rotenone for 6 h on day 0 (glucose-consuming phase) and day 5 (lactate-consuming phase). Human fibroblasts were treated with 2 μM rotenone for 16 h on day 3 (glucose-consuming phase) and day 13 (lactate-consuming phase). All cells were treated with either 2-DG/rotenone or vehicle control by supplementing the existing medium.

2.9. Cell viability MTT and LDH assays

Viability of 2-DG or rotenone treated cells was analysed using the MTT reduction and the LDH release assays. MTT was added to the existing culture medium at 480 μM for 1 h. After removal of the medium the MTT was solubilised in DMSO. The increase in absorbance at 560 nm was standardised to vehicle treated cells to account for differences in cell confluency between glucose-consuming and lactate-consuming phases. Extracellular lactate dehydrogenase (LDH) activity was determined using the LDH Cytotoxicity Detection Kit (Roche), as per manufactures instructions. Values were standardised to cells lysed in medium containing 1% (v/v) Triton X-100.

2.10. Statistical analyses

All experiments were performed with at least 3 independent repeats (n = 3) using separate cell culture samples. All data shown in graphical representations are mean values ± standard error of the mean (SEM). Statistical analyses were performed using two-way ANOVA with Bonferroni secondary testing and unpaired Students *t*-test (two-tailed) as appropriate. P-values of <0.05 were considered statistically significant. GraphPad Prism 5 software was used for all analyses.

3. Results

3.1. Depletion of medium glucose induces lactate consumption in cultured pMEFs

Under the culture conditions described, monitoring the glucose and lactate content of the pMEF culture medium revealed an initial glucose-consuming phase associated with lactate accumulation in the medium (day 0 to day 3), indicating a predominantly glycolytic phenotype (Fig. 1A). Then, once glucose in the medium had been depleted, lactate in the medium progressively declined (day 3 to day 7) indicating the cells had entered a lactate-consuming phase marked by increased reliance on mitochondrial oxidative phosphorylation (Fig. 1A). Protein levels per well, used as a surrogate marker of cell proliferation (Engelhard et al., 1991), increased rapidly during the glucose-consuming phase but then slowed once the cells entered the lactate-consuming phase (Fig. 1B). Consistent with this, the transition from glucose-consuming to lactate-consuming was accompanied by a marked decrease in protein expression of proliferating cell nuclear antigen (PCNA, Fig. 1C), an established marker of cell proliferation (Wang, 2014). Phase contrast images indicated relatively consistent pMEF morphology in both phases of the study period, despite variations in cell density (Fig. 1D).

3.2. Increased markers of mitochondrial OXPHOS during the lactate-consuming phase

The switch from net lactate production during the glucose-consuming phase to net lactate consumption once available glucose had been depleted from the culture medium (Fig. 1A) indicates an increased reliance on mitochondrial OXPHOS. To test this possibility, cells were exposed to the fluorescent probe MitoTracker Deep Red. Mitochondrial retention of MitoTracker Deep Red is dependent upon mitochondrial membrane potential (Hallap et al., 2005; Nakahira et al., 2011), and can therefore be predicted to increase in cells with increased OXPHOS. MitoTracker Deep Red fluorescence intensity increased 7-fold in pMEFs in the lactate-consuming phase when compared to cells in the glucose-consuming phase (Fig. 2A). By contrast, immunostaining for mitochondrial import receptor subunit TOM20 homolog (TOM20, Fig. 2B) and TOM20 western blot analyses (Fig. 2C) showed relative consistency, indicating that the observed increase in MitoTracker Deep Red fluorescence is not simply due to an overall increase in mitochondrial mass (Burbulla et al., 2014). To confirm that mitochondrial accumulation of MitoTracker Deep Red is dependent on mitochondrial membrane potential, pMEFs were treated with the mitochondrial depolarisation compound carbonyl cyanide *p*-(trifluoromethoxy) phenylhydrazone

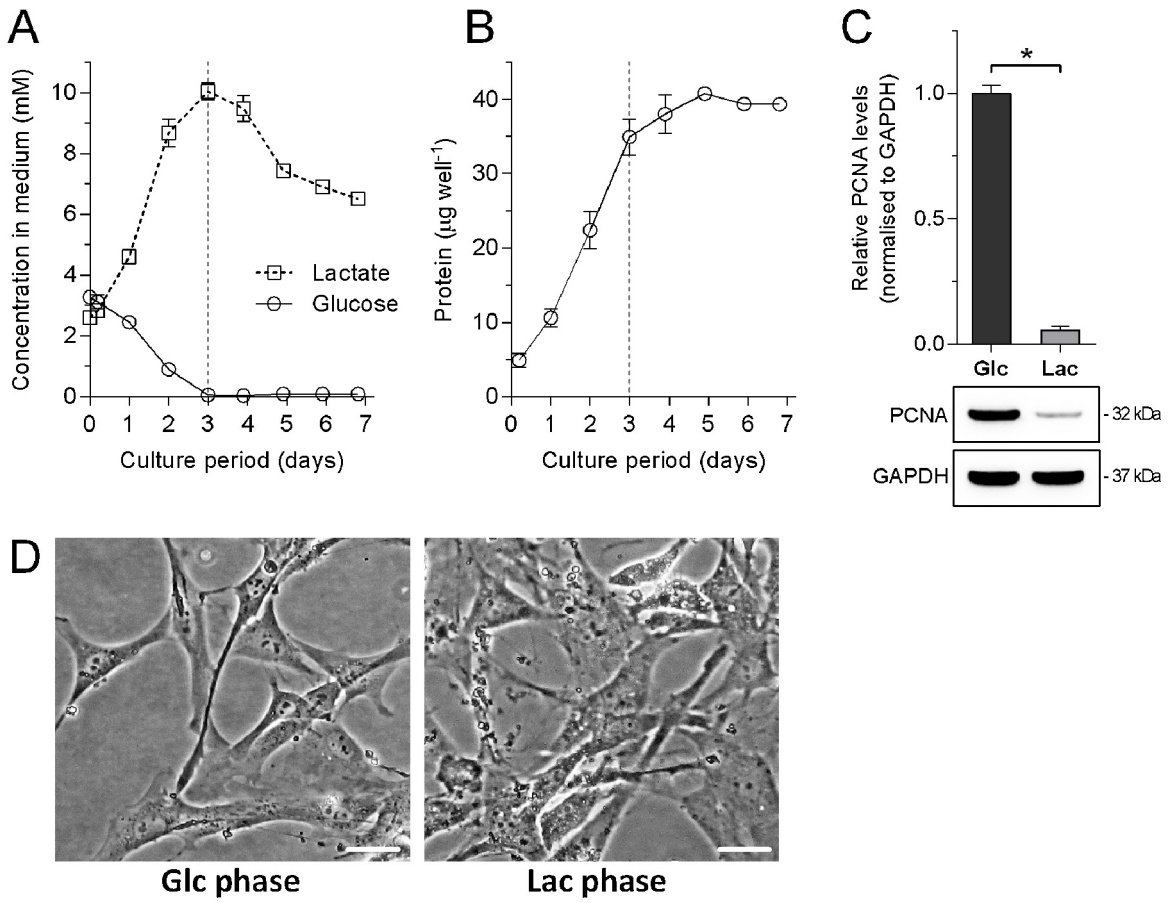

Fig. 1. Effects of medium glucose depletion on pMEF cell growth and morphology.
(A) Glucose and lactate concentration in culture medium showing two phases of growth: a glucose-consuming (glycolytic) phase during days 0–3 followed by a lactate-consuming (OXPHOS) phase. Vertical dashed lines indicate the point at which glucose in the medium is depleted. (B) Total protein content measured daily using the BCA assay. (C) Proliferating cell nuclear antigen (PCNA) levels determined by western blot for glucose-consuming cells ("Glc", day 1) and lactate-consuming cells ("Lac", day 5). Densitometry values are normalised to levels of the GAPDH loading control and are expressed relative to day 1 cells. (D) Representative phase contrast microscopy images indicating cell density and morphology for glucose-consuming cells ("Glc phase", day 1) and lactate-consuming cells ("Lac phase", day 5). Scale bar = 25 µm. * Denotes $p < 0.05$ when compared to glucose-consuming cells on day 1, unpaired Students *t*-test (n = 4).

(FCCP). Treating with FCCP decreased MitoTracker Deep Red staining intensity within the mitochondrial area (Fig. 3).

To further explore the possibility that OXPHOS is increased in pMEFs in the lactate-consuming phase, cell extracts were assessed for components of the Kreb's cycle and mitochondrial electron transport chain. These analyses revealed levels of citrate synthase, cytochrome c oxidase subunit 5 B (COX-5B), ATP synthase subunit alpha (ATP5A) and succinate dehydrogenase subunit B (SDHB) are all increased in pMEFs in the lactate-consuming phase (Fig. 4A-D). These changes are consistent with increased flux through the pathways needed to support OXPHOS in the lactate-consuming phase. Given the role for superoxide dismutase 2 (SOD2) in detoxifying mitochondrial reactive oxygen species (Flynn and Melov, 2013), increased expression of SOD2 in the lactate-consuming phase (Fig. 4E) is also consistent with increased flux through the electron transport chain. The absence of any changes to cytosolic SOD1 levels (Fig. 4F) indicates the changes to SOD2 are not due to a relatively generic increase in cellular oxidative stress associated with the transition from glucose-consuming to lactate-consuming. Moreover, levels of activated AMPKα were also unchanged (Fig. 4G). AMPKα is activated via phosphorylation at Thr172 in response to cellular energy stress (Viollet et al., 2010). Thus, the absence of any change to activated AMPKα indicates that the pMEFs are not under cellular energy stress in the lactate-consuming phase.

3.3. Cells in the lactate-consuming phase are more sensitive to rotenone

Supporting the notion that pMEFs in the glucose-consuming phase rely predominantly on glycolysis to meet their energy needs and cells in the lactate-consuming phase rely predominantly on OXPHOS, we found the cells displayed differential sensitivity to the inhibitors 2-DG and rotenone. Exposure to the glycolysis inhibitor 2-DG induced significant changes to MTT reduction and protein content per well when pMEFs were in the glucose-consuming phase yet had relatively little impact on pMEFs during the lactate-consuming phase (Fig. 5A and B). By contrast, exposing pMEFs to the OXPHOS inhibitor rotenone had a greater impact on MTT reduction, protein content per well and LDH release in the lactate-consuming phase when compared to pMEFs in the glucose-consuming phase (Fig. 5C–E). To assess whether results obtained from pMEFs could be recapitulated in other cell types, primary adult human skin fibroblasts and primary mouse brain astrocytes were also used to model the glucose-consuming and lactate-consuming phases. Specific culture conditions varied across the three cell types examined (as described in the Materials and Methods), but once these conditions were established the delineation between glucose-consuming and lactate-consuming was identified (Fig. 6A and D). Consistent with results obtained from the pMEFs, the mouse brain astrocytes (Fig. 6B and C) and the adult human skin fibroblasts

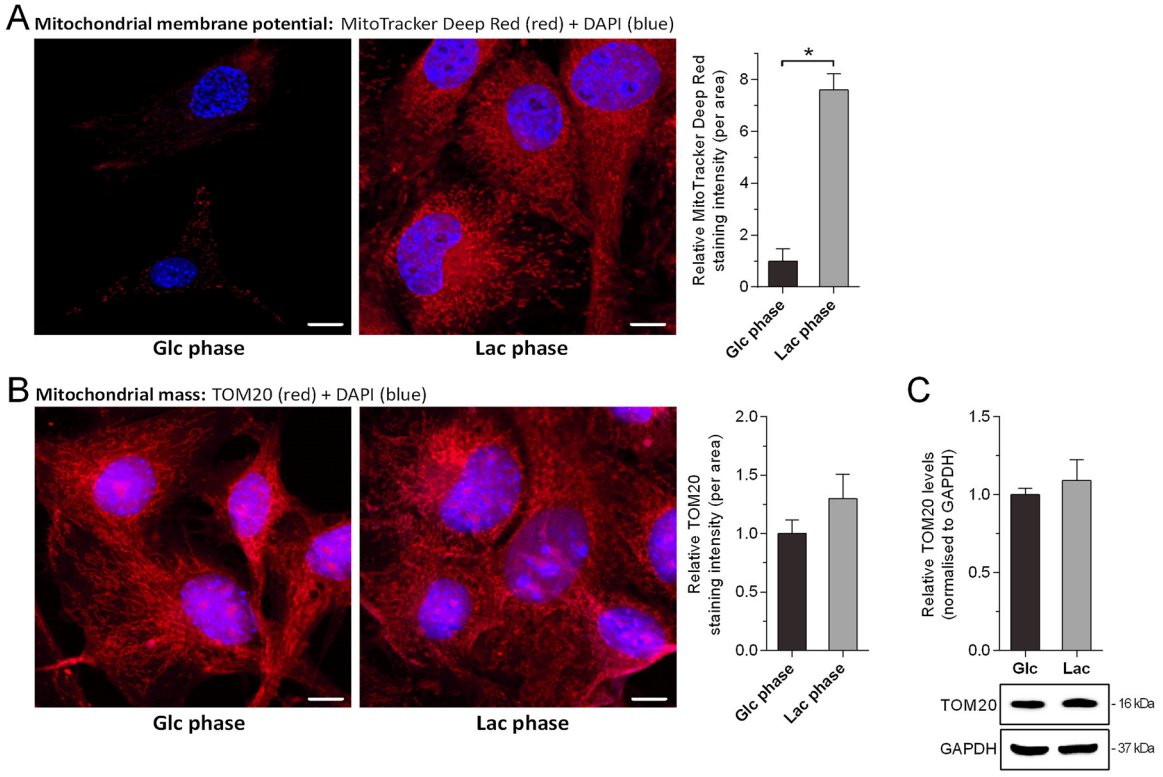

Fig. 2. MitoTracker Deep Red and TOM20 staining intensity in glucose-consuming and lactate-consuming pMEFs.
Fluorescence microscopy images showing cellular distribution of (A) a mitochondria-specific dye MitoTracker Deep Red and (B) the mitochondrial import receptor subunit TOM20 homolog (TOM20). All cells were counter stained for nuclei using DAPI (blue) and representative images for glucose-consuming cells ("Glc phase", day 1) and lactate-consuming cells ("Lac phase", day 5) taken using confocal microscopy and Zen imaging software. All cells were imaged using identical exposure times and laser power settings. Scale bar = 15 μm in A and 10 μm in B. Quantitation of MitoTracker Deep Red was derived from confocal images and quantitation of TOM20 was derived from epifluorescence images. (C) TOM20 levels determined by western blot for glucose-consuming cells ("Glc", day 1) and lactate-consuming cells ("Lac", day 5). Densitometry values are normalised to levels of the GAPDH loading control and are expressed relative to day 1 cells. * Denotes $p < 0.05$ when compared to glucose-consuming cells on day 1, unpaired Students *t*-test (n = 3-4).

(Fig. 6E and F) displayed higher sensitivity to rotenone during the lactate-consuming phase.

4. Discussion

Although glycolysis is relatively inefficient at generating ATP when compared to OXPHOS, this inefficiency can be offset by dramatically accelerating flux rates through the glycolytic pathway (Marroquin et al., 2007). Indeed, this is a central tenet of the Crabtree effect (Crabtree, 1929) whereby cells cultured in glucose-containing medium preferentially produce ATP via glycolysis despite an abundant supply of oxygen and the presence of functional mitochondria. Thus many cell types, including cancer cells, embryonically-derived cells and proliferating thymocytes, acquire highly glycolytic phenotypes when cultured in glucose-containing medium (Guppy et al., 1993; Marroquin et al., 2007; Rossignol et al., 2004; Seshagiri and Bavister, 1991). This has significant implications for cell culture studies that aim to investigate mitochondria-related processes *in vitro* because, unlike most cells in the body, cells grown in standard culture medium can readily survive independently of mitochondrial OXPHOS. A salient example of this is evident in rho^0 cells; these cells have no capacity for OXPHOS due to depletion of mitochondrial DNA yet can be grown in culture medium supplemented with sufficient glucose (King and Attardi, 1996). The highly glycolytic nature of cells cultured in glucose-containing medium therefore limits the utility of cell culture to accurately study some mitochondria-related processes *in vitro*.

The present study aimed to circumvent the Crabtree effect by developing an alternate *in vitro* model in which cells are required to rely on mitochondrial OXPHOS to meet their energy needs. To achieve this, pMEFs were grown in low glucose (3.5 mM) conditions and two phases of growth were identified: the initial glucose-consuming (glycolytic) phase followed by the lactate-consuming (OXPHOS) phase (Fig. 1A). The high rate of net lactate production compared to glucose consumption during the glycolytic phase indicates that the cells were converting almost all of the pyruvate generated during glycolysis to lactate and exporting it to the medium rather than utilising the pyruvate in mitochondrial OXPHOS (Zwingmann and Leibfritz, 2003). While the number of days required to consume all available medium glucose varied between the cell types studied, presumably due to intrinsic differences in metabolic and growth rates, none of the three cell types exhibited net lactate consumption until after all the available glucose had been depleted (Fig. 1A, 6A and 6D). This indicates that under the conditions examined these cells retain a predominantly glycolytic phenotype, in preference to OXPHOS, until glucose is no longer available. It therefore appears that the switch to dependence upon OXPHOS in these cells under the cell culture conditions described requires depletion of glucose from the medium, a condition likely to incur its own limitations. For example, glucose metabolism provides essential precursors for chemical constituents required for cell division (Hume and Weidemann, 1979; Vander Heiden et al., 2009) and the absence of glucose metabolism is therefore likely to have contributed to the observed cessation in cell proliferation once glucose in the medium had been depleted (Fig. 1B and C). Thus, utility of this cell culture model as

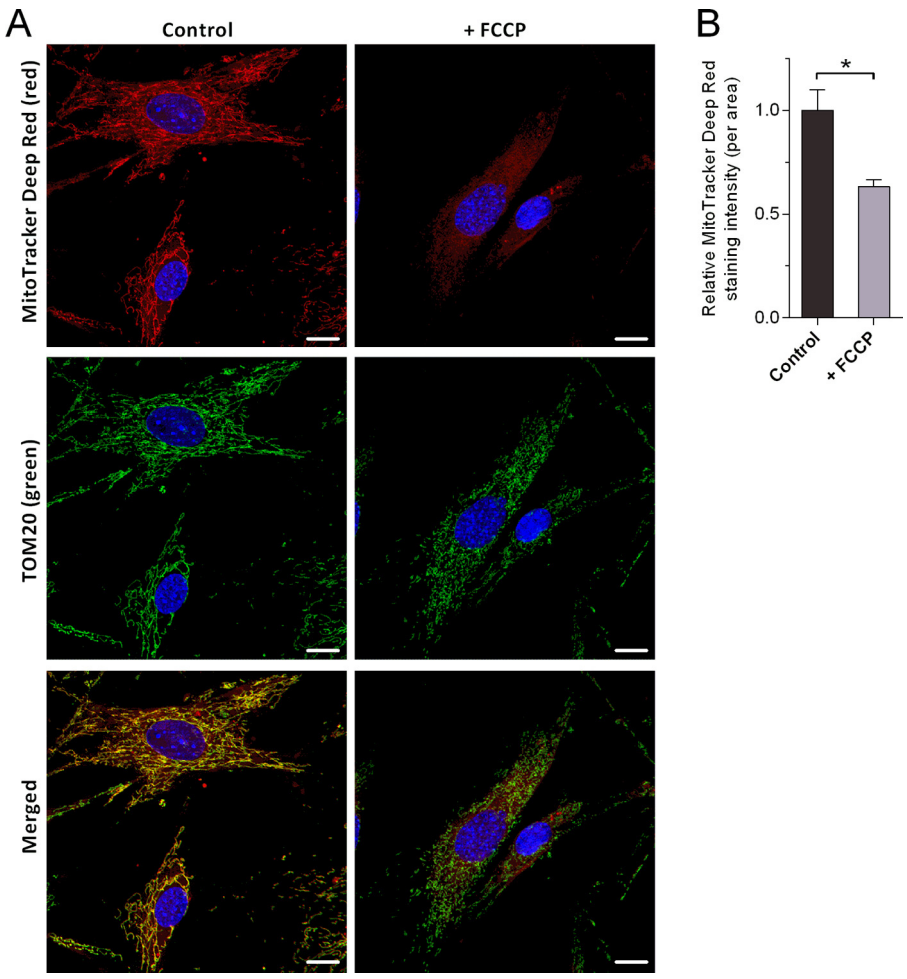

Fig. 3. Effects of the mitochondrial depolarisation compound FCCP on MitoTracker Deep Red staining intensity in pMEFs.
(A) Fluorescence microscopy images showing cellular distribution of the mitochondria-specific dye MitoTracker Deep Red (red) and the mitochondrial import receptor subunit TOM20 homolog (TOM20, green). All cells were counter stained for nuclei using DAPI (blue) and representative images for control and carbonyl cyanide p-(trifluoromethoxy) phenylhydrazone (FCCP) treated pMEFs taken using confocal microscopy and Zen imaging software. All cells were imaged using identical exposure times and laser power settings for each stain. Scale bar = 15 μm. (B) MitoTracker Deep Red staining intensity within mitochondria was quantified using TOM20 to generate a mask of the mitochondrial area and staining intensity is expressed relative to control cells. * Denotes $p < 0.05$ when compared to control cells, unpaired Students *t*-test (n = 3).

an alternate model to avoid limitations of the Crabtree effect is still dependent upon the initial glucose-consuming glycolytic phase during which the cells proliferate to sufficient levels to support subsequent analyses.

These limitations are avoided in the galactose model in which glycolytic pathways can still support cell proliferation while the slow oxidation of galactose to pyruvate drives dependence upon OXPHOS, as indicated by decreased medium lactate levels in galactose cultured cells (Aguer et al., 2011; Altamirano et al., 2006). However, culturing cells in galactose can introduce alternate limitations. For example, some cell types (e.g. skeletal muscle cells) are unable to metabolise galactose (Elkalaf et al., 2013; Mailloux and Harper, 2010) and galactose can induce an accelerated ageing phenotype in both *in vitro* and *in vivo* contexts (Barker et al., 1999; Choi et al., 2013; Coban et al., 2014; Li et al., 2014). Further to this, AMPK is recognised for its central role in regulating cellular energy levels via phosphorylation at Thr172 in response to cellular energy stress (Viollet et al., 2010), and previous studies have shown increased pAMPKα in galactose cultured cells, suggesting that galactose in the medium can induce a state of cellular energy stress (Aguer et al., 2011). By contrast, the current study shows pAMPKα levels are unchanged in the lactate-consuming phase (Fig. 4G), suggesting that the predominately oxidative cells in this phase are under no additional cellular energy stress when compared to cells in the glucose-consuming phase.

Mitochondrial uptake and retention of the fluorescent probe MitoTracker Deep Red is influenced by mitochondrial membrane potential and the reducing environment of active mitochondria (Hallap et al., 2005; Nakahira et al., 2011). Relative to TOM20 levels, which indicated total mitochondrial mass (Burbulla et al., 2014) within the cells was not affected by the transition from the glucose-consuming phase to the lactate-consuming phase (Fig. 2B and C), MitoTracker Deep Red staining indicated a substantial increase in mitochondrial membrane potential during the lactate-consuming phase (Fig. 2A). These data suggest that increased MitoTracker Deep Red staining intensity in the lactate-consuming cells is not confounded by changes in mitochondrial mass and that mitochondria during the lactate-consuming phase are relatively more active when compared to the mitochondria during the glucose-consuming phase. Moreover, the 7-fold increase in MitoTracker Deep Red staining intensity observed when cells switched from glucose-consuming to lactate-consuming (Fig. 2A) appears to exceed the magnitude in changes to membrane potential measured when cells cultured in glucose-containing medium are exposed to conditions expected to have a strong impact upon mitochondrial membrane potential (Appleby et al., 1999; Buchet and Godinot, 1998). Thus, monitoring changes to mitochondrial functionality,

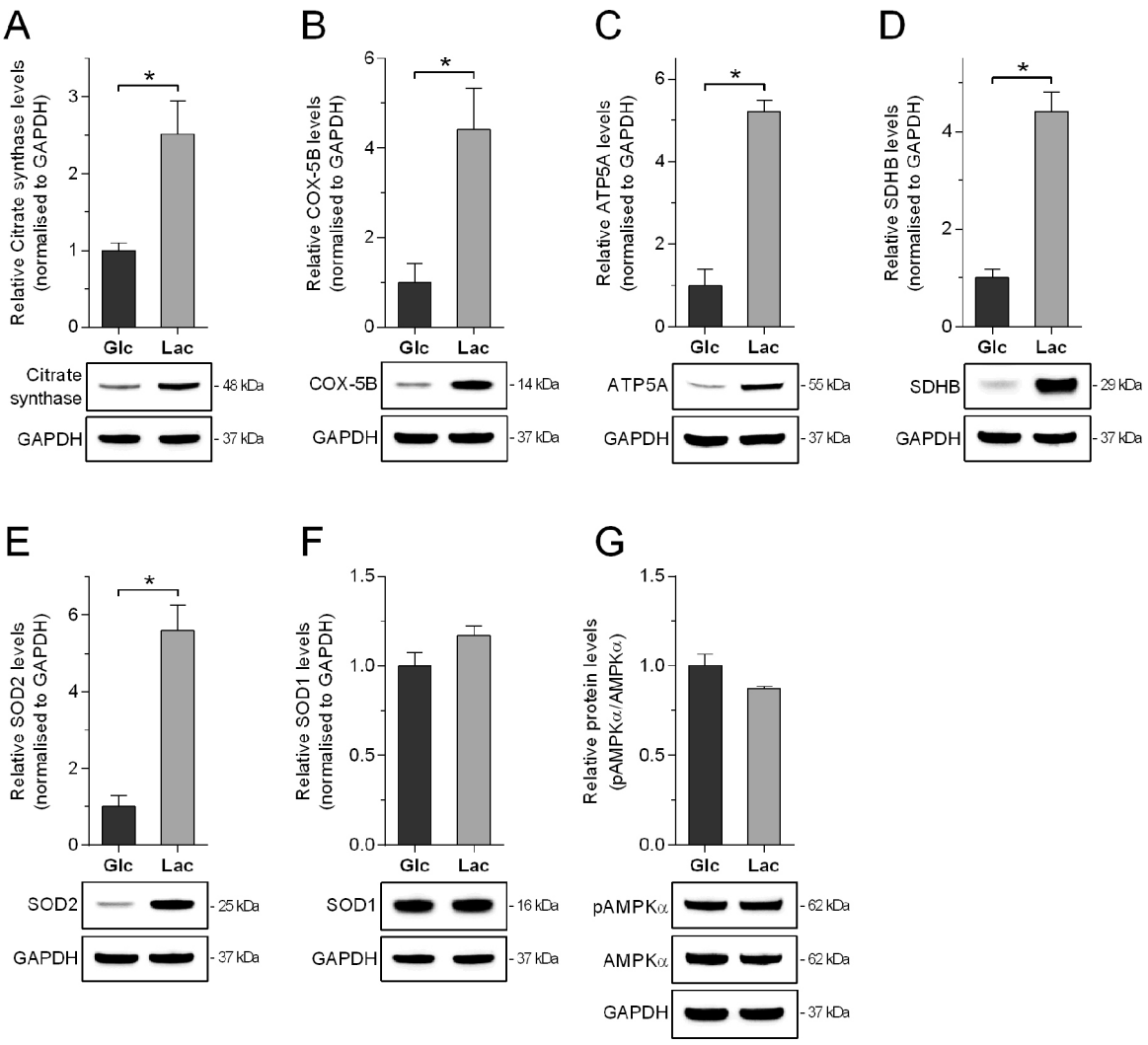

Fig. 4. Expression of mitochondrial proteins and AMPKα in glucose-consuming and lactate-consuming pMEFs.
(A) Citrate synthase levels, (B) cytochrome c oxidase subunit 5 B (COX-5B) levels, (C) ATP synthase subunit alpha (ATP5A) levels, (D) succinate dehydrogenase subunit B (SDHB) levels, (E) superoxide dismutase 2 (SOD2) levels, (F) superoxide dismutase 1 (SOD1) levels, (G) phosphorylated (Thr172) 5′-adenosine monophosphate-activated protein kinase alpha (pAMPKα) levels and total AMPKα levels determined by western blot for glucose-consuming cells ("Glc", day 1) and lactate-consuming cells ("Lac", day 5). Densitometry values are normalised to levels of the GAPDH loading control and are expressed relative to day 1 cells. * Denotes $p < 0.05$ when compared to glucose-consuming cells on day 1, unpaired Students *t*-test (n = 3–4).

such as changes to membrane potential, appears to be substantially influenced by whether or not the cells are primarily consuming substrates that favour reliance on glycolysis over OXPHOS.

Increased mitochondrial membrane potential in the lactate-consuming phase is consistent with increased expression of electron transport chain subunit proteins COX5B, ATP5A, and SDHB (Fig. 4B, C and D) and previous studies that have demonstrated suppressed OXPHOS in glucose cultured cells (Golshani-Hebroni and Bessman, 1997; Rodriguez-Enriquez et al., 2001). COX5B plays a crucial role in complex IV assembly and expression levels of this protein are related to mitochondrial membrane potential and mitochondrial ability to generate ATP, such that COX5B deficient cells are unable to grow in galactose-containing medium (Galati et al., 2009). ATP5A forms part of the catalytic core of ATP synthase, which plays a central role in controlling flux through the oxidative phosphorylation pathway (Nilsson and Nielsen, 2016). Likewise, increased SDHB expression levels (Fig. 4D) are associated with increased mitochondrial ATP production (Matsumoto et al., 2012), and increased expression of citrate synthase (Fig. 4A), a pace-making enzyme of the Krebs cycle, is consistent with increased citrate synthase activity seen in galactose cultured cells (Aguer et al., 2011). These data are also consistent with increased SOD2 expression levels seen in lactate-consuming cells (Fig. 4E), given the role for SOD2 in detoxifying reactive oxygen species within mitochondria (Flynn and Melov, 2013) and previous studies which have reported lower levels of SOD2 in glycolytic cancer cells (Bize et al., 1980).

A metabolic switch from reliance on glycolysis during the glucose-consuming phase to reliance on OXPHOS during the lactate-consuming phase is supported by the heightened sensitivity of glucose-consuming cells to the glycolysis inhibitor 2-DG (Fig. 5A and B) and increased sensitivity of lactate-consuming cells to the OXPHOS inhibitor rotenone (Figs. 5C, D, E, 6B, C, E and F). These data demonstrate that despite differences in tissue of origin (central nervous system versus periphery) or species of origin, all cell types examined showed significantly increased sensitivity to an OXPHOS inhibitor during the lactate-consuming phase. This indicates the potential utility of this model when assessing compounds that may have mitochondrial toxic properties; in order to gain full understanding of a compound that may exhibit inhibitory activity towards mitochondrial ATP generation it will be pertinent

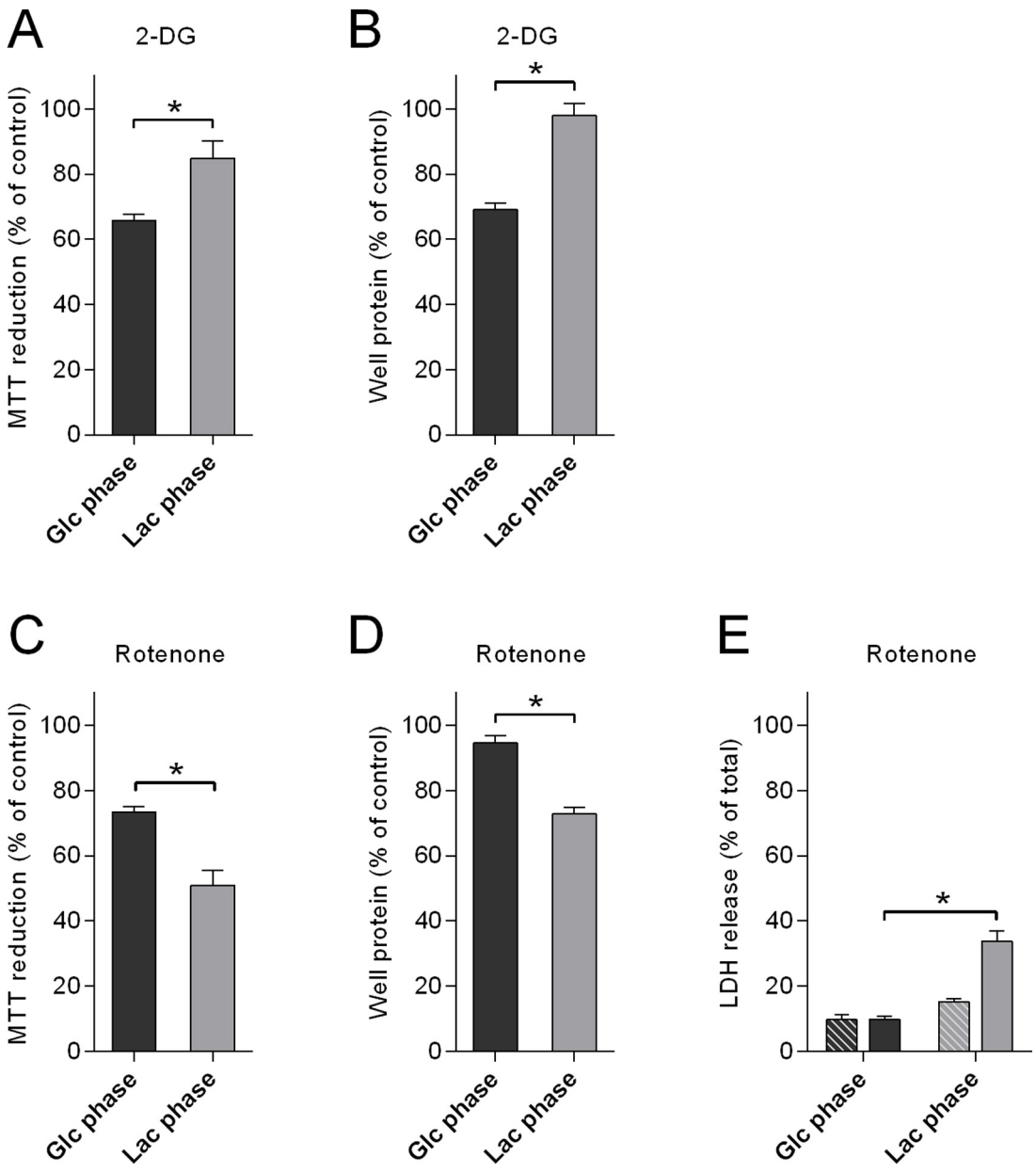

Fig. 5. Effects of the glycolysis inhibitor 2-deoxyglucose and the OXPHOS inhibitor rotenone on pMEFs under glucose-consuming and lactate-consuming culture conditions. Effects of the glycolysis inhibitor 2-deoxyglucose (2-DG, 5 mM, 24 h) on glucose-consuming ("Glc phase", day 1) and lactate-consuming ("Lac phase", day 5) pMEFs assessed using (A) cell viability MTT reduction assay and (B) total protein per well. Effects of the OXPHOS inhibitor rotenone (100 μM, 4 h) on glucose-consuming ("Glc phase", day 1) and lactate-consuming ("Lac phase", day 5) pMEFs assessed using (C) cell viability MTT reduction assay, (D) total protein per well and (E) cell viability LDH release assay. Data in A-D are expressed relative to vehicle control treated cells at the respective glucose-consuming or lactate-consuming phases of growth. Data in E are expressed relative to total LDH released following lysis with Triton X-100 where hashed bars indicate vehicle control treated cells and non-hashed bars indicate rotenone treated cells. * Denotes $p < 0.05$ when compared to glucose-consuming cells on day 1, unpaired Students ($n = 3$-8) for A–D or two-way ANOVA with Bonferroni secondary testing ($n = 8$) for E.

to use cells with a higher dependence upon OXPHOS than cells that are primarily glycolytic (Dott et al., 2014; Marroquin et al., 2007).

An additional potential utility of this model may relate to mimicking the energy metabolism of cells which, *in vivo*, have higher energy requirements relative to other cells. As an example, neurons in the central nervous system are more inherently reliant upon OXPHOS for the supply of their energy needs with very limited capacity to up-regulate glycolysis (Belanger et al., 2011; Herrero-Mendez et al., 2009). According to the astrocyte-neuron lactate shuttle hypothesis (ANLSH), the high energy demand of neurons is supported by astrocytes which supply neurons with lactate (Pellerin et al., 2007). Similarly, recent studies show that oligodendrocytes also metabolically support neurons *in vivo* (Funfschilling et al., 2012; Lee et al., 2012). Thus, the lactate-consuming phase of this model may have some utility in replicating the *in vivo* reliance of neurons on lactate. Furthermore, a recent study has shown that differentiation of pluripotent stem cells into motor neurons involves a decrease in glycolytic flux and increased expression of mitochondrial respiratory chain subunits despite no apparent change in overall mitochondrial mass (O'Brien et al., 2015). The latter of these observations is consistent with the increase in Mito-Tracker Deep Red fluorescence intensity in the lactate-consuming pMEFs despite no change in TOM20 levels (Fig. 2). Conversely, reprograming somatic cells into induced pluripotent stem cells requires a shift from oxidative to glycolytic metabolism (Mathieu et al., 2014). These results therefore highlight the importance of

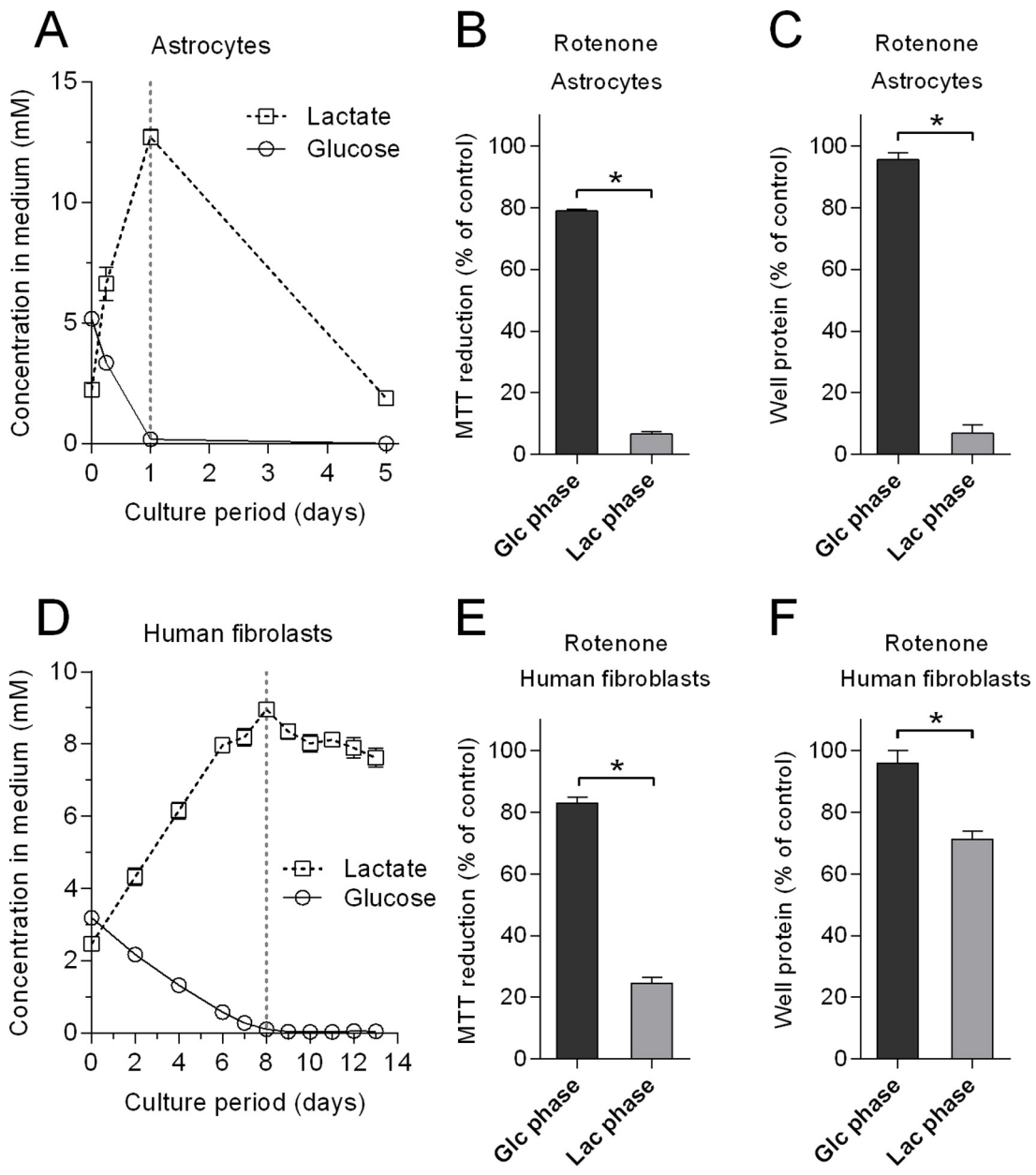

Fig. 6. Effects of the OXPHOS inhibitor rotenone on multiple cell types under glucose-consuming and lactate-consuming culture conditions.
(A) Glucose and lactate concentration in the culture medium of primary mouse brain astrocytes showing a glucose-consuming phase during days 0–1 followed by a lactate-consuming phase. Effects of the OXPHOS inhibitor rotenone (50 nM, 6 h) on glucose-consuming ("Glc phase", day 0) and lactate-consuming ("Lac phase", day 5) astrocytes assessed using (B) cell viability MTT reduction assay and (C) total protein per well. (D) Glucose and lactate concentration in the culture medium of primary adult human skin fibroblasts showing a glucose-consuming phase during days 0–8 followed by a lactate-consuming phase. Effects of rotenone (2 μM, 16 h) on glucose-consuming ("Glc phase", day 3) and lactate-consuming ("Lac phase", day 13) human fibroblasts assessed using (E) cell viability MTT reduction assay and (F) total protein per well. Vertical dashed lines indicate the point at which glucose in medium is depleted. Data in B–C and E–F are expressed relative to vehicle control treated cells at the respective glucose-consuming or lactate-consuming phases of growth. * Denotes $p < 0.05$ when compared to glucose-consuming cells on day 1, unpaired Students ($n = 3$-6).

considering the metabolic state of cells (glycolytic vs. oxidative) not only when attempting to investigate conditions with an expected immediate impact upon mitochondrial function (e.g. toxin studies) but also when investigating cell types known to have a naturally higher oxidative metabolic phenotype.

5. Conclusion

Herein are described *in vitro* cell culture conditions in which cell autonomous depletion of glucose from the culture medium forces cells to utilise lactate via mitochondrial OXPHOS to supply their energy needs. While this model presents its own considerable caveats (i.e. reliance upon complete depletion of glucose from the medium) and does not address other significant non-physiological elements of culturing cells under commonly used conditions (e.g. atmospheric oxygen concentrations), it nonetheless provides alternate opportunity to study cellular processes and diseases involving the mitochondrion without limitations incurred via the Crabtree effect.

Conflict of interest

The authors declare that they have no conflicts of interest.

Acknowledgements

We thank Ian Blair and Garth Nicholson for providing the adult human fibroblast cells. Confocal microscopy was performed using facilities at the Biological Optical Microscopy Platform (BOMP), University of Melbourne. This work was supported by funds from the Motor Neurone Disease Research Institute of Australia, the National Health and Medical Research Council, and the University of Melbourne. The funders had no role in study design, data collection and analysis, decision to publish, or preparation of the manuscript.

References

Aguer, C., Gambarotta, D., Mailloux, R.J., Moffat, C., Dent, R., Mcpherson, R., Harper, M.E., 2011. Galactose enhances oxidative metabolism and reveals mitochondrial dysfunction in human primary muscle cells. PLoS One 6, e28536.

Allen, S.P., Rajan, S., Duffy, L., Mortiboys, H., Higginbottom, A., Grierson, A.J., Shaw, P.J., 2014. Superoxide dismutase 1 mutation in a cellular model of amyotrophic lateral sclerosis shifts energy generation from oxidative phosphorylation to glycolysis. Neurobiol. Aging 35, 1499–1509.

Altamirano, C., Illanes, A., Becerra, S., Cairo, J.J., Godia, F., 2006. Considerations on the lactate consumption by CHO cells in the presence of galactose. J. Biotechnol. 125, 547–556.

Appleby, R.D., Porteous, W.K., Hughes, G., James, A.M., Shannon, D., Wei, Y.H., Murphy, M.P., 1999. Quantitation and origin of the mitochondrial membrane potential in human cells lacking mitochondrial DNA. Eur. J. Biochem. 262, 108–116.

Barker, M.G., Brimage, L.J., Smart, K.A., 1999. Effect of Cu,Zn superoxide dismutase disruption mutation on replicative senescence in Saccharomyces cerevisiae. FEMS Microbiol. Lett. 177, 199–204.

Belanger, M., Allaman, I., Magistretti, P.J., 2011. Brain energy metabolism: focus on astrocyte-neuron metabolic cooperation. Cell Metab. 14, 724–738.

Bird, M.J., Wijeyeratne, X.W., Komen, J.C., Laskowski, A., Ryan, M.T., Thorburn, D.R., Frazier, A.E., 2014. Neuronal and astrocyte dysfunction diverges from embryonic fibroblasts in the Ndufs4fky/fky mouse. Biosci. Rep. 34, e00151.

Bize, I.B., Oberley, L.W., Morris, H.P., 1980. Superoxide dismutase and superoxide radical in Morris hepatomas. Cancer Res. 40, 3686–3693.

Buchet, K., Godinot, C., 1998. Functional F1-ATPase essential in maintaining growth and membrane potential of human mitochondrial DNA-depleted rho degrees cells. J. Biol. Chem. 273, 22983–22989.

Burbulla, L.F., Fitzgerald, J.C., Stegen, K., Westermeier, J., Thost, A.K., Kato, H., Mokranjac, D., Sauerwald, J., Martins, L.M., Woitalla, D., Rapaport, D., Riess, O., Proikas-Cezanne, T., Rasse, T.M., Kruger, R., 2014. Mitochondrial proteolytic stress induced by loss of mortalin function is rescued by Parkin and PINK1. Cell. Death. Dis. 5, e1180.

Choi, J.H., Kim, D.W., Yoo, D.Y., Jeong, H.J., Kim, W., Jung, H.Y., Nam, S.M., Kim, J.H., Yoon, Y.S., Choi, S.Y., Hwang, I.K., 2013. Repeated administration of PEP-1-Cu,Zn-superoxide dismutase and PEP-1-peroxiredoxin-2 to senescent mice induced by D-galactose improves the hippocampal functions. Neurochem. Res. 38, 2046–2055.

Coban, J., Betul-Kalaz, E., Kucukgergin, C., Aydin, A.F., Dogan-Ekici, I., Dogru-Abbasoglu, S., Uysal, M., 2014. Blueberry treatment attenuates D-galactose-induced oxidative stress and tissue damage in rat liver. Geriatr. Gerontol. Int. 14, 490–497.

Crabtree, H.G., 1929. Observations on the carbohydrate metabolism of tumours. Biochem. J. 23, 536–545.

Dott, W., Mistry, P., Wright, J., Cain, K., Herbert, K.E., 2014. Modulation of mitochondrial bioenergetics in a skeletal muscle cell line model of mitochondrial toxicity. Redox Biol. 2, 224–233.

Elkalaf, M., Andel, M., Trnka, J., 2013. Low glucose but not galactose enhances oxidative mitochondrial metabolism in C2C12 myoblasts and myotubes. PLoS One 8, e70772.

Engelhard 3rd, H.H., Krupka, J.L., Bauer, K.D., 1991. Simultaneous quantification of c-myc oncoprotein, total cellular protein: and DNA content using multiparameter flow cytometry. Cytometry 12, 68–76.

Flynn, J.M., Melov, S., 2013. SOD2 in mitochondrial dysfunction and neurodegeneration. Free Radic. Biol. Med. 62, 4–12.

Funfschilling, U., Supplie, L.M., Mahad, D., Boretius, S., Saab, A.S., Edgar, J., Brinkmann, B.G., Kassmann, C.M., Tzvetanova, I.D., Mobius, W., Diaz, F., Meijer, D., Suter, U., Hamprecht, B., Sereda, M.W., Moraes, C.T., Frahm, J., Goebbels, S., Nave, K.A., 2012. Glycolytic oligodendrocytes maintain myelin and long-term axonal integrity. Nature 485, 517–521.

Galati, D., Srinivasan, S., Raza, H., Prabu, S.K., Hardy, M., Chandran, K., Lopez, M., Kalyanaraman, B., Avadhani, N.G., 2009. Role of nuclear-encoded subunit Vb in the assembly and stability of cytochrome c oxidase complex: implications in mitochondrial dysfunction and ROS production. Biochem. J. 420, 439–449.

Garfield, A.S., 2010. Derivation of primary mouse embryonic fibroblast (PMEF) cultures. Methods Mol. Biol. 633, 19–27.

Golshani-Hebroni, S.G., Bessman, S.P., 1997. Hexokinase binding to mitochondria: a basis for proliferative energy metabolism. J. Bioenerg. Biomembr. 29, 331–338.

Guppy, M., Greiner, E., Brand, K., 1993. The role of the Crabtree effect and an endogenous fuel in the energy metabolism of resting and proliferating thymocytes. Eur. J. Biochem. 212, 95–99.

Hallap, T., Nagy, S., Jaakma, U., Johannisson, A., Rodriguez-Martinez, H., 2005. Mitochondrial activity of frozen-thawed spermatozoa assessed by MitoTracker Deep Red 633. Theriogenology 63, 2311–2322.

Hare, D.J., Grubman, A., Ryan, T.M., Lothian, A., Liddell, J.R., Grimm, R., Matsuda, T., Doble, P.A., Cherny, R.A., Bush, A.I., White, A.R., Masters, C.L., Roberts, B.R., 2013. Profiling the iron: copper and zinc content in primary neuron and astrocyte cultures by rapid online quantitative size exclusion chromatography-inductively coupled plasma-mass spectrometry. Metallomics 5, 1656–1662.

Herrero-Mendez, A., Almeida, A., Fernandez, E., Maestre, C., Moncada, S., Bolanos, J.P., 2009. The bioenergetic and antioxidant status of neurons is controlled by continuous degradation of a key glycolytic enzyme by APC/C-Cdh1. Nat. Cell Biol. 11, 747–752.

Hume, D.A., Weidemann, M.J., 1979. Role and regulation of glucose metabolism in proliferating cells. J. Natl. Cancer Inst. 62, 3–8.

Imamura, T., Crespi, C.L., Thilly, W.G., Brunengraber, H., 1982. Fructose as a carbohydrate source yields stable pH and redox parameters in microcarrier cell culture. Anal. Biochem. 124, 353–358.

King, M.P., Attardi, G., 1996. Isolation of human cell lines lacking mitochondrial DNA. Methods Enzymol. 264, 304–313.

Lee, Y., Morrison, B.M., Li, Y., Lengacher, S., Farah, M.H., Hoffman, P.N., Liu, Y., Tsingalia, A., Jin, L., Zhang, P.W., Pellerin, L., Magistretti, P.J., Rothstein, J.D., 2012. Oligodendroglia metabolically support axons and contribute to neurodegeneration. Nature 487, 443–448.

Li, Y.N., Guo, Y., Xi, M.M., Yang, P., Zhou, X.Y., Yin, S., Hai, C.X., Li, J.G., Qin, X.J., 2014. Saponins from Aralia taibaiensis attenuate D-galactose-induced aging in rats by activating FOXO3a and Nrf2 pathways. Oxid. Med. Cell Longev., 320513.

Liddell, J.R., Zwingmann, C., Schmidt, M.M., Thiessen, A., Leibfritz, D., Robinson, S.R., Dringen, R., 2009. Sustained hydrogen peroxide stress decreases lactate production by cultured astrocytes. J. Neurosci. Res. 87, 2696–2708.

Lunt, S.Y., Vander Heiden, M.G., 2011. Aerobic glycolysis: meeting the metabolic requirements of cell proliferation. Annu. Rev. Cell Dev. Biol. 27, 441–464.

Mailloux, R.J., Harper, M.E., 2010. Glucose regulates enzymatic sources of mitochondrial NADPH in skeletal muscle cells; a novel role for glucose-6-phosphate dehydrogenase. FASEB J. 24, 2495–2506.

Marroquin, L.D., Hynes, J., Dykens, J.A., Jamieson, J.D., Will, Y., 2007. Circumventing the Crabtree effect: replacing media glucose with galactose increases susceptibility of HepG2 cells to mitochondrial toxicants. Toxicol. Sci. 97, 539–547.

Mathieu, J., Zhou, W., Xing, Y., Sperber, H., Ferreccio, A., Agoston, Z., Kuppusamy, K.T., Moon, R.T., Ruohola-Baker, H., 2014. Hypoxia-inducible factors have distinct and stage-specific roles during reprogramming of human cells to pluripotency. Cell Stem Cell 14, 592–605.

Matsumoto, S., Uchiumi, T., Tanamachi, H., Saito, T., Yagi, M., Takazaki, S., Kanki, T., Kang, D., 2012. Ribonucleoprotein Y-box-binding protein-1 regulates mitochondrial oxidative phosphorylation (OXPHOS) protein expression after serum stimulation through binding to OXPHOS mRNA. Biochem. J. 443, 573–584.

Nakahira, K., Haspel, J.A., Rathinam, V.A., Lee, S.J., Dolinay, T., Lam, H.C., Englert, J.A., Rabinovitch, M., Cernadas, M., Kim, H.P., Fitzgerald, K.A., Ryter, S.W., Choi, A.M., 2011. Autophagy proteins regulate innate immune responses by inhibiting the release of mitochondrial DNA mediated by the NALP3 inflammasome. Nat. Immunol. 12, 222–230.

Nilsson, A., Nielsen, J., 2016. Metabolic trade-offs in yeast are caused by F1F0-ATP synthase. Sci. Rep. 6, 22264.

O'Brien, L.C., Keeney, P.M., Bennett Jr., J.P., 2015. Differentiation of human neural stem cells into motor neurons stimulates mitochondrial biogenesis and decreases glycolytic flux. Stem Cells Dev. 4, 1984–1994.

Pellerin, L., Bouzier-Sore, A.K., Aubert, A., Serres, S., Merle, M., Costalat, R., Magistretti, P.J., 2007. Activity-dependent regulation of energy metabolism by astrocytes: an update. Glia 55, 1251–1262.

Robinson, B.H., Petrova-Benedict, R., Buncic, J.R., Wallace, D.C., 1992. Nonviability of cells with oxidative defects in galactose medium: a screening test for affected patient fibroblasts. Biochem. Med. Metab. Biol. 48, 122–126.

Rodriguez-Enriquez, S., Juarez, O., Rodriguez-Zavala, J.S., Moreno-Sanchez, R., 2001. Multisite control of the Crabtree effect in ascites hepatoma cells. Eur. J. Biochem. 268, 2512–2519.

Rossignol, R., Gilkerson, R., Aggeler, R., Yamagata, K., Remington, S.J., Capaldi, R.A., 2004. Energy substrate modulates mitochondrial structure and oxidative capacity in cancer cells. Cancer Res. 64, 985–993.

Seshagiri, P.B., Bavister, B.D., 1991. Glucose and phosphate inhibit respiration and oxidative metabolism in cultured hamster eight-cell embryos: evidence for the crabtree effect. Mol. Reprod. Dev. 30, 105–111.

Solski, J.A., Yang, S., Nicholson, G.A., Luquin, N., Williams, K.L., Fernando, R., Pamphlett, R., Blair, I.P., 2012. A novel TARDBP insertion/deletion mutation in the flail arm variant of amyotrophic lateral sclerosis. Amyotroph. Lateral Scler. 13, 465–470.

Vander Heiden, M.G., Cantley, L.C., Thompson, C.B., 2009. Understanding the Warburg effect: the metabolic requirements of cell proliferation. Science 324, 1029–1033.

Vichai, V., Kirtikara, K., 2006. Sulforhodamine B colorimetric assay for cytotoxicity screening. Nat. Protoc. 1, 1112–1116.

Viollet, B., Horman, S., Leclerc, J., Lantier, L., Foretz, M., Billaud, M., Giri, S., Andreelli, F., 2010. AMPK inhibition in health and disease. Crit. Rev. Biochem. Mol. Biol. 45, 276–295.
Wang, S.C., 2014. PCNA: a silent housekeeper or a potential therapeutic target. Trends Pharmacol. Sci. 35, 178–186.
Warburg, O., Geissler, A.W., Lorenz, S., 1967. [On growth of cancer cells in media in which glucose is replaced by galactose]. Hoppe. Seylers Z. Physiol. Chem. 348, 1686–1687.
Zwingmann, C., Leibfritz, D., 2003. Regulation of glial metabolism studied by 13C-NMR. NMR Biomed. 16, 370–399.